NASA Contractor Report 198297 (Corrected Copy Dec. 1996)

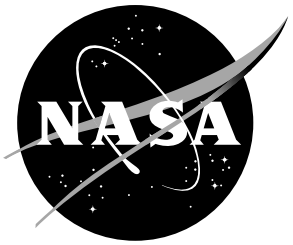

Turbulent Wall-Pressure Fluctuations: New Model for Off-Axis Cross-Spectral Density

Bart A. Singer
High Technology Corporation, Hampton, Virginia

Contract NAS1-20059

March 1996

National Aeronautics and
Space Administration
Langley Research Center
Hampton, Virginia 23681-0001

Abstract

Models for the distribution of the wall-pressure under a turbulent boundary layer often estimate the coherence of the cross-spectral density in terms of a product of two coherence functions. One such function describes the coherence as a function of separation distance in the mean-flow direction, the other function describes the coherence in the cross-stream direction. Analysis of data from a large-eddy simulation of a turbulent boundary layer reveals that this approximation dramatically underpredicts the coherence for separation directions that are neither aligned with nor perpendicular to the mean-flow direction. These models fail even when the coherence functions in the directions parallel and perpendicular to the mean flow are known exactly. A new approach for combining the parallel and perpendicular coherence functions is presented. The new approach results in vastly improved approximations for the coherence.

1 Introduction

Reduced levels of aircraft interior cabin noise are desirable for both comfort and health-related reasons. Blake [1] notes that a turbulent boundary layer on the fuselage at locations forward of the engines dominates the excitation of the fuselage structure. Boeing 737 flight experiments by Wilby and Gloyna [2] confirm the importance of turbulent boundary-layer pressure fluctuations on the noise level inside the aircraft cabin. Innovative use of fuselage materials and arrangement of the frames and stringers provides some opportunity for a reduction in the amount of vibration transmitted to the interior cabin. However, in order to design such a structure, detailed information with regard to wall-pressure fluctuations in the external turbulent boundary layer is required.

Although the importance of the desired information is clear, a thorough mapping of the wall-pressure fluctuations under a turbulent boundary layer is difficult to obtain experimentally. The size of the pressure transducer influences the temporal response [3, 4, 5], and the noise level and frequency range in the experimental facility must be taken into account [5, 6]. Direct numerical simulation and large-eddy simulation (LES) were first used to obtain wall-pressure fluctuation statistics for low-Reynolds-number channel flows [7, 8].

Efforts to model the turbulent wall-pressure fluctuations have been hampered by the lack of an extensive and reliable database. The validity of many reasonable assumptions made in various models could not be adequately tested with available data. This situation has begun to change with a recent LES by Singer [9] of a turbulent boundary layer with a Reynolds number based on a displacement thickness of 3500. The extensive dataset allows for a more careful evaluation of reasonable modeling assumptions. In particular, this paper will address a common assumption known as the "multiplication hypothesis" in which the coherence of the cross-spectral density for an arbitrary separation direction is formed by the product of the cross-spectral densities for streamwise and spanwise separations, respectively. A comparison of the data from the LES with that predicted from the multiplication hypothesis will show that this assumption is inadequate. A new approach that requires no additional data will be introduced and will be shown to be more accurate than the previous model.

2 The Generic Problem

Figure 1 shows a plan view of the wall under a turbulent boundary layer. The mean flow travels in the x direction; the spanwise direction is denoted by y. The wall pressure at an arbitrary spatial location and at an arbitrary time t is $p(x, y, t)$. A second arbitrary wall-pressure is $p(x + \xi, y + \eta, t + \tau)$, where ξ and η are the separation distances in the x and y directions, respectively, and τ is a time separation between the two measurements. If the flow is homogeneous in x, y, and t, the two-point correlation depends only on the separations in space and time and can be written as a convolution integral:

$$R(\xi, \eta, \tau) = \frac{1}{L_x\, L_y\, T} \int_0^{L_x} \int_0^{L_y} \int_0^{T} p(x, y, t) p(x + \xi, y + \eta, t + \tau)\, dx\, dy\, dt \tag{1}$$

where L_x, L_y, and T are the domain lengths in x, y, and t. If the data are assumed to be homogeneous in all three variables, then the correlation is independent of the values of x, y, and t. In a generic flat-plate turbulent boundary layer, the homogeneity assumption is exact in y and t but only approximate in x. The growth of the boundary layer in the x direction accounts for a mild inhomogeneity; the fact that the boundary-layer growth occurs over distances that are long relative to typical correlation distances results in approximate homogeneity. In the LES of Singer [9], the numerical approach enforces streamwise homogeneity of the flow.

The pressure data can be investigated in the frequency domain by taking the Fourier transform of the two-point correlation,

$$\Gamma(\xi, \eta, \omega) = \mathcal{F}\{R(\xi, \eta, \tau)\} \tag{2}$$

where $\mathcal{F}$ implies a Fourier transform. We use the standard nomenclature of the community of wall-pressure investigators and call the function $\Gamma(\xi, \eta, \omega)$ the cross-spectral density. In general, the cross-spectral density is a complex-valued function. However, the autospectrum

$$\phi(\omega) = \Gamma(0, 0, \omega) \tag{3}$$

is strictly real. Experimental determination of the autospectrum is a much simpler process than the determination of the full cross-spectral density function because the former only requires measurements at a single position and the latter requires a two-dimensional array of measurements. In order of decreasing availability, experiments have been performed that measure:

1. $\phi(\omega)$
2. $\Gamma(\xi, 0, \omega)$
3. $\Gamma(\xi, 0, \omega)$ and $\Gamma(0, \eta, \omega)$
4. $\Gamma(\xi, \eta, \omega)$ (usually for only a few values of η/ξ)

The recent availability of numerical simulation data can be expected to fill some of the gaps in our knowledge of the wall pressure distribution.

3 Previous Model

The model of Corcos [3, 10, 11] has been used in various forms for more than 3 decades. The model expresses the cross-spectral density function as a product of simpler functions; that is,

$$\Gamma(\xi, \eta, \omega) = \phi(\omega) A(\xi, \omega) B(\eta, \omega) \exp(-\iota\alpha) \tag{4}$$

where $A(\xi, \omega)$ and $B(\eta, \omega)$ are real-valued functions that represent the coherences in the longitudinal and lateral directions, respectively, and all of the phase information is contained in α. Corcos made two important contributions with Eq. (4). The first is the general form of the cross-spectral density function as a product of simpler functions that can be individually determined (the multiplication hypothesis). The second contribution provides similarity forms for the functions $A(\xi, \omega)$ and $B(\eta, \omega)$. In this work, we address only the first aspect of the generalized Corcos model. In other words, does the multiplication hypothesis as defined in Eq. (4) provide the proper framework for modeling the full cross-spectral density function?

4 Comparison of LES Data with Model Predictions

For comparison of the model predictions with the LES data, we normalize the magnitude of the cross-spectral density function with the autocorrelation to obtain a coherence function

$$\gamma(\xi, \eta, \omega) \equiv |\Gamma(\xi, \eta, \omega)|/\phi(\omega) = A(\xi, \omega) B(\eta, \omega) \tag{5}$$

This work is concerned with the validity of the form of Eq. (5) and not the particular functions used to represent $\phi(\omega)$, $A(\xi, \omega)$, and $B(\eta, \omega)$; hence, the numerical values of $\phi(\omega)$, $A(\xi, \omega)$, and $B(\eta, \omega)$ will be taken directly from the LES data; that is,

$$A(\xi, \omega) = |\Gamma(\xi, 0, \omega)|/\phi(\omega) \tag{6}$$

$$B(\eta, \omega) = |\Gamma(0, \eta, \omega)|/\phi(\omega) \tag{7}$$

and $\phi(\omega)$ is determined from Eq. (3). By evaluating the functions $\phi(\omega)$, $A(\xi, \omega)$, and $B(\eta, \omega)$ directly from the LES data, the comparison of the off-axis (both ξ and η nonzero) coherence will be the best that the multiplication hypothesis of Eq. (5) can produce.

Figure 2 shows contours of the left- and right-hand sides of Eq. (5) for a specific frequency $\omega\delta^*/u_\tau = 8.98$, where δ^* is the displacement thickness and u_τ is the friction velocity. The solid lines represent the values of the coherence that are determined directly from the LES; the dashed lines represent the product $A(\xi, \omega)B(\eta, \omega)$, which has been traditionally used to model the coherence. The product formulation produces nearly straight contour lines; the contour lines of the actual coherence are curved like ellipses. Even though the values of the coherence are chosen to exactly match for $\xi = 0$ and $\eta = 0$, the product formulation exhibits large errors for off-axis combinations of ξ and η. Similar problems occur at other frequencies.

5 A New Model

The elliptical shape of the contours of $\gamma(\xi, \eta, \omega)$ from the LES suggests that the coherence might be more appropriately modeled in a modified polar coordinate system. To develop such

a coordinate system, we first seek a scaling relation for the independent variables ($\xi = s\eta$) such that the A and B curves are similar. In the general case treated here, each frequency is separately considered; hence, the scaling factor $s(\omega)$ is a function of frequency. The determination of the scaling factor for a particular frequency involves the minimization of the error

$$E(s,\omega) = \int_0^{\xi_{\text{cutoff}}} [A(\xi,\omega) - B(\xi/s,\omega)]^2 \, d\xi \tag{8}$$

Alternatively, the integration could be taken over η by replacing ξ with $s\eta$ in Eq. (8). The cutoff value for the integration limit must be chosen to ensure that data are available for the evaluation of both $A(\xi_{\text{cutoff}},\omega)$ and $B(\xi_{\text{cutoff}}/s,\omega)$. An example of an optimized fit from the LES data is illustrated in Fig. 3. The value of ξ_{cutoff} was chosen to be the maximum value of ξ for which data for A were available; in the figure, $\xi_{\text{cutoff}}/\delta^* \approx 22$. In a case for which data are available for very large values of ξ, a useful value for the cutoff would be the greatest value of ξ for which the coherence $A(\xi,\omega)$ first becomes insignificant.

If the functions A and B are taken to be one-dimensional functions of similarity variables (for example, if $A = A(\xi\omega/U_c)$ and $B = B(\eta\omega/U_c)$, where U_c is the convection velocity), then the scaling factor needs to be determined for only a single frequency; the factor for other frequencies can be determined analytically. In addition, if exponential forms are used to represent both A and B, then the scaling factor can be derived by straightforward analysis.

After the scaling function $s(\omega)$ has been obtained, radial and azimuthal coordinates are developed. The radial coordinate is

$$r = \sqrt{\xi^2 + (s\eta)^2} \tag{9}$$

and the azimuthal coordinate is

$$\theta = \arctan(s\eta/\xi) \tag{10}$$

As η goes to 0, the radial coordinate r goes to ξ and the angular coordinate θ goes to 0. Hence, small perturbations away from a strictly streamwise separation produce a smooth departure of r from ξ. Similarly, as ξ tends to 0, the radial coordinate r tends to $s\eta$ and θ goes to $\pi/2$. If the correspondence between $A(\xi,\omega)$ and $B(\xi/s,\omega)$ were perfect (for example, if both functions were exponentials), then a suitable approximation for the off-axis coherence would be a function of the radial coordinate r only. In such a circumstance, both $A(r,\omega)$ and $B(r/s,\omega)$ would be identical; either could be used to model $\gamma(\xi,\eta,\omega)$. In the more general case, only an approximate relationship exists between $A(\xi,\omega)$ and $B(\xi/s,\omega)$. In this more general case, $A(r,\omega)$ is expected to be a more accurate approximation when η is small, and $B(r/s,\omega)$ is expected to be more accurate when ξ is small. Hence, a reasonable estimate for the coherence shifts the major contribution from $A(r,\omega)$ to $B(r/s,\omega)$ as $s\eta$ increases relative to ξ. The proposed new model introduces a linear fit to represent the shifting contribution; that is,

$$\gamma(\xi,\eta,\omega) = A(r,\omega) + (B(r/s,\omega) - A(r,\omega))2\theta/\pi \tag{11}$$

Contours of the coherence predicted by the new model for $\omega\delta^*/u_\tau = 8.98$ are indicated by the dashed lines in Fig. 4. The agreement of the new model with the LES data is improved dramatically compared with the model used in Fig. 2. Similarly, an improved agreement exists for other frequencies, as illustrated in Figs. 5(a)–(h).

6 Simplified Implementations

The new model for the off-axis coherence is a simple and straightforward improvement over the formulation of Eq. (5), which employs a product of the longitudinal and lateral coherences. The new model can easily be incorporated into existing computer codes with minimal programming effort. No new data are required, although new measurements of the longitudinal and lateral coherences can easily be exploited to obtain more accurate predictions. The subsections below detail simplified implementations of the new model into current algorithms that use various assumptions with regard to the form of the coherences A and B.

6.1 Coherences depend upon similarity variables

In this case $A = A(\alpha)$ and $B = B(\beta)$, where α and β are similarity variables. In the usual case $\alpha = \xi\omega/U_c$ and $\beta = \eta\omega/U_c$, where α is related to the phase of the cross-spectral density function and U_c is the convection velocity. Because the coherences depend only on single variables, the optimal scaling parameter s is a constant and is defined by the minimization of

$$E(s) = \int_0^{\alpha_{\text{cutoff}}} [A(\alpha) - B(\alpha/s)]^2 \, d\alpha \tag{12}$$

where α_{cutoff} must be great enough to ensure that $A(\alpha_{\text{cutoff}})$ and $B(\alpha_{\text{cutoff}}/s)$ are defined. A reasonable choice of α_{cutoff} results in values of $A(\alpha_{\text{cutoff}})$ and $B(\alpha_{\text{cutoff}}/s)$ that are near the lower limit of significance. Greater values of α_{cutoff} cause the integral in Eq. (12) to accumulate large contributions from regions in which the coherence is small. The determination of $A(\alpha)$ and $B(\beta)$ can be performed with either algebraic expressions, function calls, or table lookups. After s has been obtained, Eqs.(9), (10), and (11) can be used instead of the product formulation (Eq. (5)).

6.2 A and B represented by the same functional form

In this case, the scaling parameter can be found analytically. Typically, in this case, A and B are single variable functions; however, this requirement is not necessary. The scaling parameter s is chosen to make

$$A(\xi) \equiv B(\xi/s) \tag{13}$$

As an example, in the model of Efimtsov [12]:

$$A(\xi, \Lambda_\xi) = \exp\left(-\xi/\Lambda_\xi\right) \tag{14}$$

and

$$B(\eta, \Lambda_\eta) = \exp\left(-\eta/\Lambda_\eta\right) \tag{15}$$

where Λ_ξ and Λ_η are correlation lengths that depend upon the frequency and various flow parameters. In order to satisfy Eq. (13), s must be chosen so that

$$\exp\left(-\xi/\Lambda_\xi\right) = \exp\left(-(\xi/s)/\Lambda_\eta\right) \tag{16}$$

which requires

$$s = \Lambda_\xi/\Lambda_\eta \tag{17}$$

For the Efimtsov model, although s will always equal the ratio Λ_ξ/Λ_η, the specific numerical values of s will vary with the frequency and flow conditions because the values of Λ_ξ and Λ_η vary with the frequency and flow conditions. As in the previous subsections, after s has been obtained, Eqs.(9), (10), and (11) can be used instead of the product formulation (Eq. (5)).

7 Conclusions

A large-eddy simulation database was used to evaluate the validity of the multiplication hypothesis for modeling the coherence of the cross-spectral density of the wall-pressure fluctuations. Comparison with the data from the numerical simulation revealed that even under optimal conditions the use of the multiplication hypothesis predicts off-axis coherences that are badly in error. A new modeling form was introduced and shown to perform much more accurately. The new model requires no additional data than that previously used, and the implementation of the new model into existing computer codes can be readily achieved. For instances in which various simplifying assumptions in regard to the form of the longitudinal and lateral coherences have been exploited in an existing computer program, shortcuts for the inclusion of the new modeling form were discussed.

8 Acknowledgments

The author thanks Dr. Craig Streett for many useful suggestions. This work was carried in the Fluid Mechanics and Acoustics Division of NASA Langley Research Center under contract NAS1-20059.

References

[1] Blake, W., *Mechanics of Flow-Induced Sound and Vibration*, Vol. II, Academic Press, p. 644 (1986).

[2] Wilby, J. F. and Gloyna, F. L., "Vibration measurements of an airplane fuselage structure: 1. Turbulent boundary layer excitation," *J. Sound and Vibration* **25**, 443 (1972).

[3] Corcos, G. M., "Resolution of pressure in turbulence," *The J. of the Acoustical Soc. of America* **35**, 192 (1963).

[4] Schewe, G., "On the structure and resolution of wall-pressure fluctuations associated with turbulent boundary-layer flow," *J. Fluid. Mech.* **134**, 311 (1983).

[5] Farabee, T. M. and Casarella, M. J., "Spectral features of wall pressure fluctuations beneath turbulent boundary layers," *Phys. Fluids A* **3**, 2410 (1991).

[6] Bull, M. K., "Properties of the fluctuating wall-pressure field of a turbulent boundary layer," AGARD Report 455 (1963).

[7] Choi, H. and Moin, P., "On the space-time characteristics of wall-pressure fluctuations," *Phys. Fluids A* **2**, 1450 (1990).

[8] Chang, P. A., Abraham, B. M., and Piomelli, U., "Wavenumber-frequency characteristics of wall pressure fluctuations computed using turbulence simulations," Presented at Symposium on Active/Passive Control of Flow-Induced Vibration and Noise: 1994 International Mechanical Engineering Congress and Exposition (1994).

[9] Singer, B. A., "Large-eddy simulation of turbulent wall-pressure fluctuations," NASA CR-198276 February (1996).

[10] Corcos, G. M., "The structure of the turbulent pressure field in boundary-layer flows," *J. Fluid Mech.* **18**, 353 (1963).

[11] Corcos, G. M., "The resolution of turbulent pressures at the wall of a boundary layer," *J. Sound Vib.* **6**, 59 (1967).

[12] Efimtsov, B. M., "Characteristics of the field of turbulent wall pressure fluctuations at large Reynolds numbers," *Sov. Phys. Acoust.* **28**, 289 (1982).

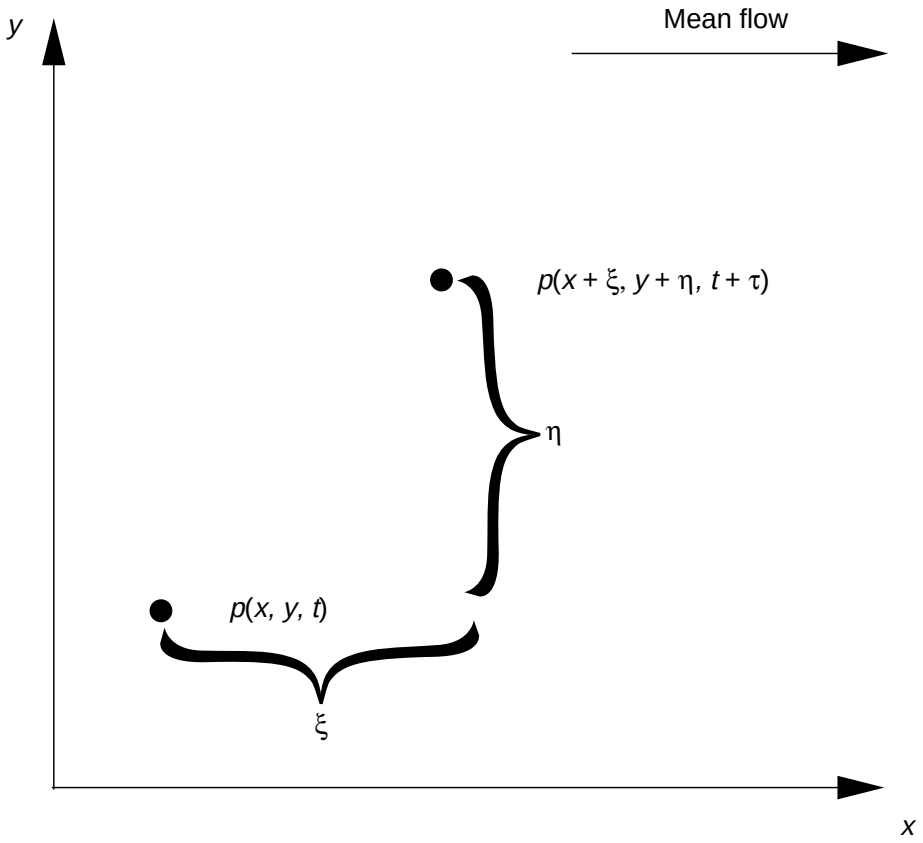

Figure 1. Plan view of boundary layer.

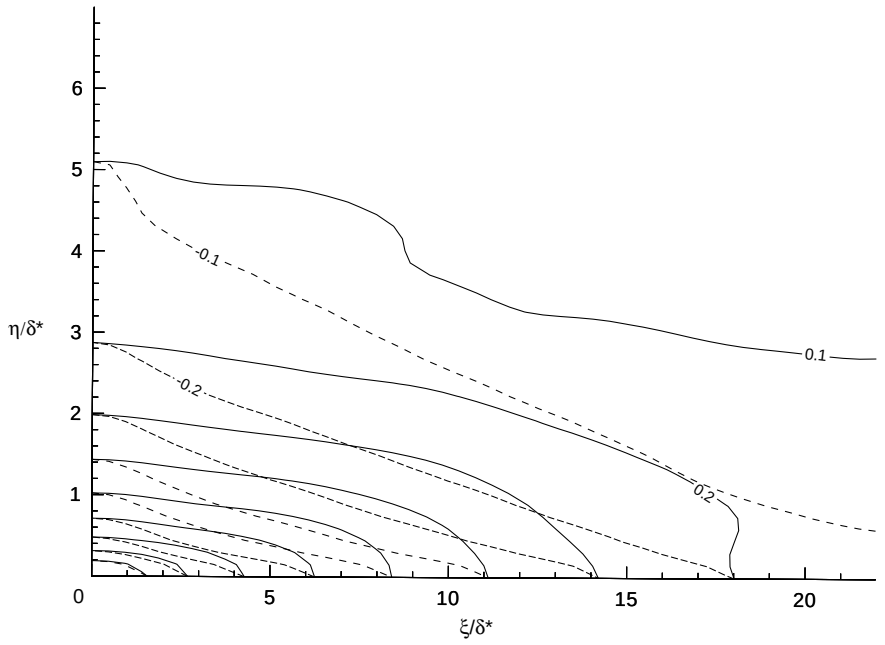

Figure 2. Coherence contours of cross-spectral density for $\omega\delta^*/u_\tau = 8.98$. Contours are spaced with increments of 0.1. _____LES data (left-hand side of Eq. (5)); _ _ _ _ _ Results from multiplication hypothesis (right-hand side of Eq. (5)).

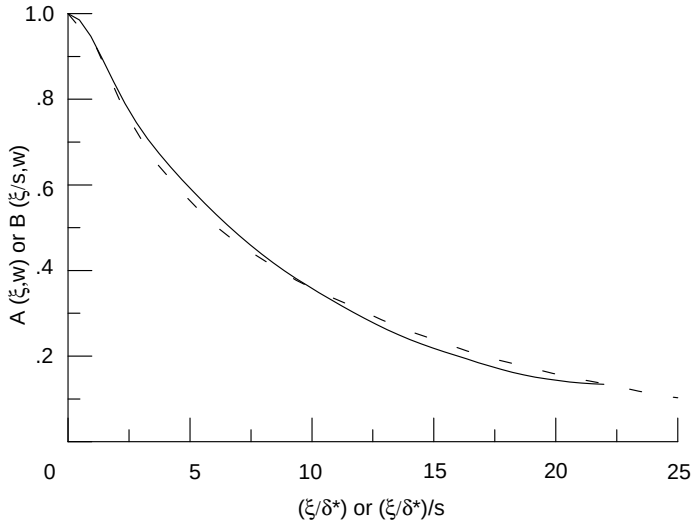

Figure 3. Comparison of $A(\xi,\omega)$ and $B(\xi/s,\omega)$ for $\omega\delta^*/u_\tau = 8.98$. Optimized value of s is 7.86. _____$A(\xi,\omega)$; . . . . . $B(\xi/s,\omega)$.

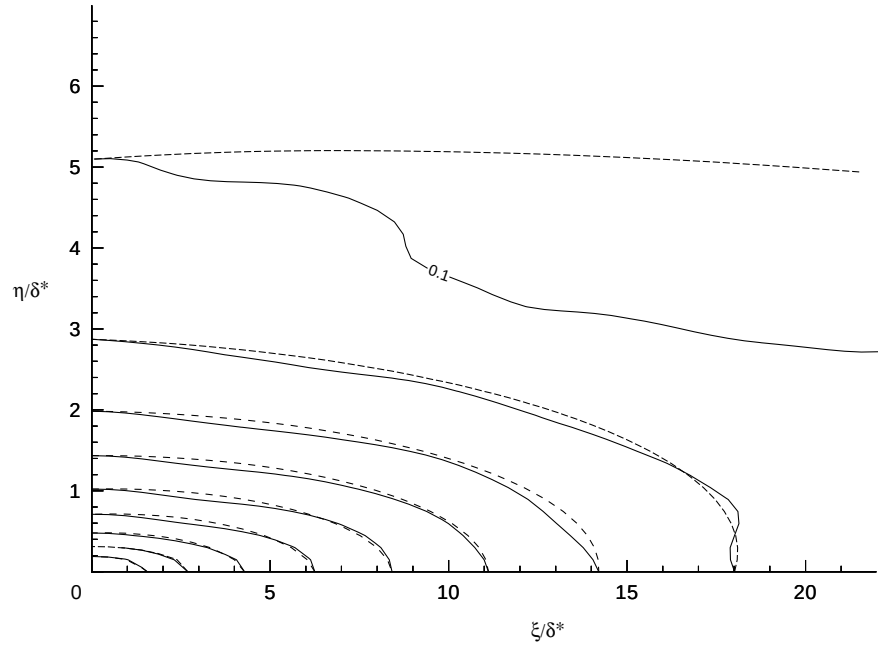

Figure 4. Coherence contours of cross-spectral density for $\omega\delta^*/u_\tau = 8.98$. Contours are spaced with increments of 0.1. _____LES data (left-hand side of Eq. (11)); _ _ _ _ _ New model (right-hand side of Eq. (11)).

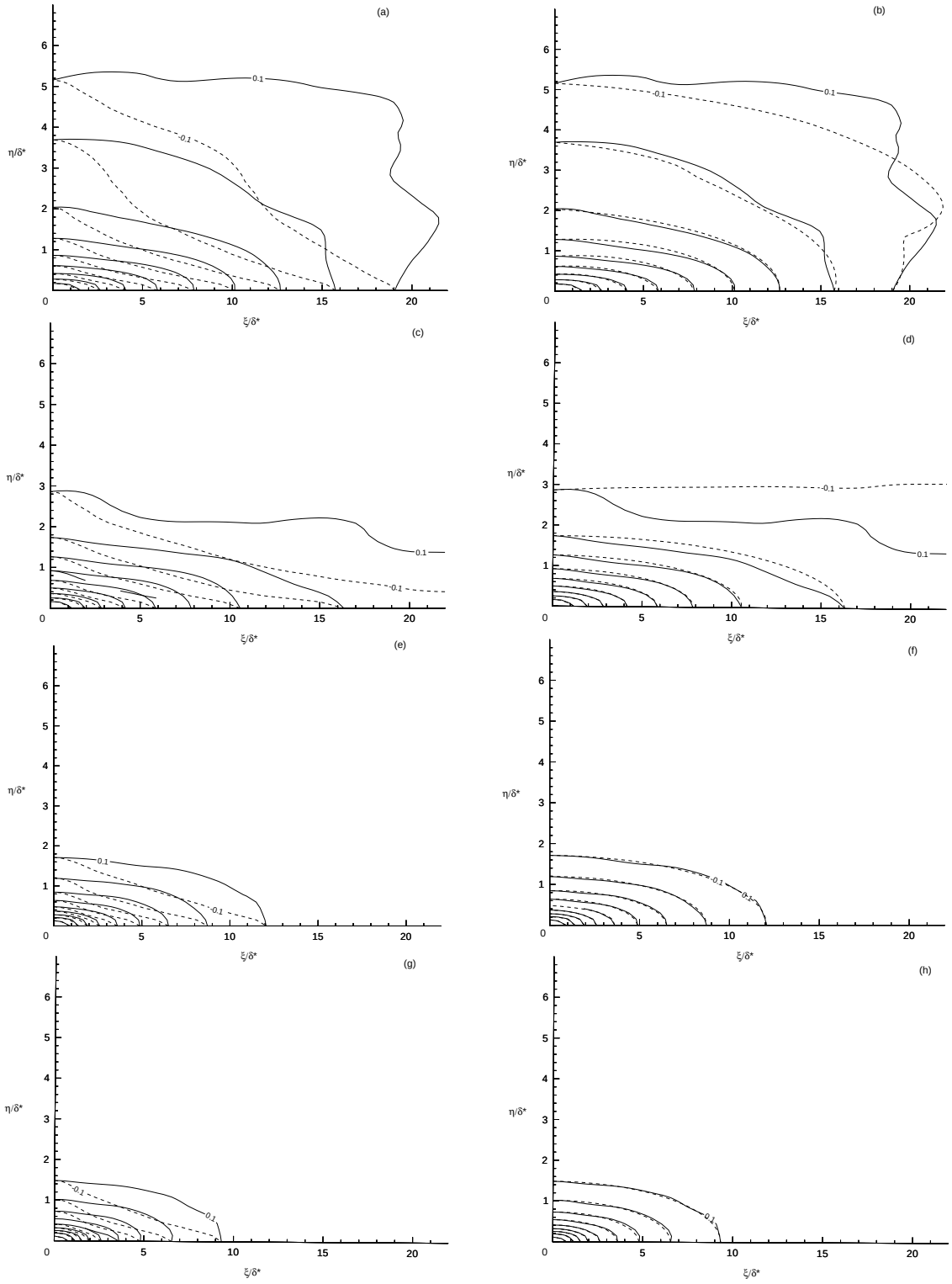

Figure 5. Coherence contours with increments of 0.1; _____LES data. _ _ _ _ _ Old or new model. a) $\omega\delta^*/u_\tau = 6.74$; Old model. b) $\omega\delta^*/u_\tau = 6.74$; New model. c) $\omega\delta^*/u_\tau = 13.48$; Old model. d) $\omega\delta^*/u_\tau = 13.48$; New model. e) $\omega\delta^*/u_\tau = 20.21$; Old model. f) $\omega\delta^*/u_\tau = 20.21$; New model. g) $\omega\delta^*/u_\tau = 26.95$; Old model. h) $\omega\delta^*/u_\tau = 26.95$; New model.